Accepted Manuscript

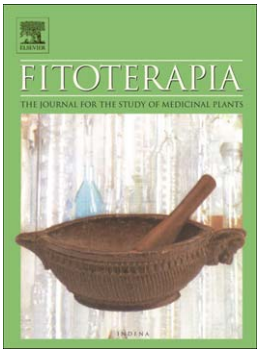

Isolation and identification of metabolites of bakuchiol in rats

Pei-le Wang, Feng-xiang Zhang, Zuo-cheng Qiu, Zhi-hong Yao, Man-sau Wong, Xin-sheng Yao, Yi Dai

PII: S0367-326X(15)30114-3
DOI: doi: 10.1016/j.fitote.2015.11.006
Reference: FITOTE 3292

To appear in: *Fitoterapia*

Received date: 11 September 2015
Revised date: 10 November 2015
Accepted date: 13 November 2015

Please cite this article as: Pei-le Wang, Feng-xiang Zhang, Zuo-cheng Qiu, Zhi-hong Yao, Man-sau Wong, Xin-sheng Yao, Yi Dai, Isolation and identification of metabolites of bakuchiol in rats, *Fitoterapia* (2015), doi: 10.1016/j.fitote.2015.11.006

Isolation and identification of metabolites of bakuchiol in rats

Pei-le Wang [a], Feng-xiang Zhang [b], Zuo-cheng Qiu [b,c], Zhi-hong Yao [b], Man-sau Wong[c], Xin-sheng Yao [a,b,*], Yi Dai [b,*]

[a] *College of Traditional Chinese Materia Medica, Shenyang Pharmaceutical University, Shenyang 110016, China*

[b] *Institute of Traditional Chinese Medicine and Natural Products, College of Pharmacy, Jinan University, Guangzhou 510632, China*

[c] *Department of Applied Biology and Chemical Technology, The Hong Kong Polytechnic University, Kowloon, Hong Kong, China*

** Correspondence to: Prof. Dr. Xin-sheng Yao, College of Traditional Chinese Materia Medica, Shenyang Pharmaceutical University, China. Tel: +86 24 23993884; fax: +86 24 23993994, E-mail: tyaoxs@jnu.edu.cn; Associate Prof. Dr. Yi Dai, College of Pharmacy, Jinan University, China. Tel: +86 20 85220785; fax: +86 20 85221559 E-mail: daiyi1004@163.com.*

Abstract

Bakuchiol, the main active component of *Psoralea corylifolia*, showed a range of significant pharmacological activities, including antimicrobial, antiinflammatory, reduction of bone loss and estrogenic activities. In this research, 12 metabolites, including 11 new compounds, were isolated from the urine and feces of rats after oral administration of bakuchiol, and their structures were elucidated by extensive spectroscopic analysis. The possible metabolic pathways of bakuchiol in rats were proposed, and a rare bile acid conjugation reaction was found. In addition, bakuchiol and its metabolites M1-M3 were studied for their alkaline phosphatase (ALP) activities on MC3T3-E1 cells and cytotoxicity on HKC-8 cells. The data showed that bakuchiol exerted significant effects on ALP activity of MC3T3-E1 cells and cytotoxicity on HKC-8 cells, while M1-M3 only showed ALP activities at 10^{-5} M on MC3T3-E1 cells and no cytotoxicity on HKC-8 cells.

Keywords:

Bakuchiol

Psoralea corylifolia

Metabolites

MC3T3-E1 cell ALP activity

HKC-8 cytotoxicity

1. Introduction

Bakuchiol, a prenylated phenolic monoterpene, is the main active component of *Psoralea corylifolia* that has been widely used in China to treat various diseases, such as psoriasis, vitiligo, osteoporosis, arthralgia and asthma [1]. It has attracted an increasing interest for its antitumor, antimicrobial, inhibition of iNOS expression, antiinflammatory, antipyretic, reduction of bone loss and estrogenic activities [2-8]. Moreover, bakuchiol showed cytotoxicity on HK-2 cells (human renal tubular epithelial cells), and high doses of bakuchiol could induce kidney toxicity in mice [9,10]. Pharmacokinetic studies reported that bakuchiol possessed poor absorption, significant first-pass metabolism, and low bioavailability [10,11]. In our previous *in vivo* study, one primary oxidized metabolite and 18 metabolites of bakuchiol were identified in biosamples by UPLC/Q-TOF-MS [12]. As the chemical structures of metabolite isomers were difficult to be deduced by liquid chromatography-tandem mass spectrometry analysis [13,14], and bioactivity evaluation needed pure compounds, the isolation of metabolites were of necessary. In order to better understanding of *in vivo* metabolism and pharmacological activity of bakuchiol, metabolites in feces and urine after oral administration to rats were isolated and identified. The ALP activity on MC3T3-E1 cells and cytotoxicity on HKC-8 cells of bakuchiol as well as its main metabolites were also evaluated.

2. Experimental

2.1. Materials

CD spectra were recorded on JASCO J-810 spectrometer. Optical rotations were

measured on JASCO P-1020 spectrometer. 1D and 2D NMR spectra were measured on a Bruker AV-400/600 spectrometer. HRESIMS data were determined by a Waters Synapt G2 mass spectrometer. Preparative HPLC performed on Shimadzu LC-6AD system equipped with a Shimadzu SPD-20A UV detector (210 nm and 260 nm), and a Welch material XB-C18 (21.2 × 250 mm) column (with a flow rate of 8 mL/min) and a Welch material XB-C18 (10 × 250 mm) column (with a flow rate of 3 mL/min) were used. Silica gel (200-300 mesh, Qingdao Haiyang Chemical Group Corp., Qingdao, China), HP-20 macroporous resin (Diaion, Japan), Sephadex LH-20 (50 μm, Amersham Pharmacia Biotech, Sweden) and ODS (50 μm, YMC, Japan) were used for open column chromatography (CC). Thin-layer chromatography (TLC) was performed using precoated silica gel plates (silica gel GF254, 1 mm, Yantai). Bakuchiol was purchased from Shanghai Ronghe Medical Technological Limited Company (Shanghai, China), and the purity was more than 98% determined by HPLC analysis.

2.2. Animals

Male Sprague-Dawley rats (250 ± 20 g) were obtained from Medical Experimental Animal Center of Guangdong Province (Guangzhou, China). They were housed at ambient temperature of 20 ± 2°C with 12-h light/dark cycles for two weeks before experiment and were fed a standard diet and water ad libitum. The animals were fasted with free access water in metabolic cages separately over night before experiment. Bakuchiol (12 g) was given to rats (32 animals) by gavage at the dose of 100 mg/kg/day in turn (three days gavaged and three days fed a standard diet, six days as a circle). Urine and feces samples were collected for 24 h after each administration from animals housed in stainless steel

metabolism cages equipped with a urine and feces separator. These samples were stored at −20 °C. The animal protocols were approved by the Guide for the Care and Use of Laboratory Animals of Jinan University. All procedures were in accordance with Guide for the Care and Use of Laboratory Animals (National Institutes of Health).

2.3. Extraction and isolation

A total of 12 L urine was collected, after condensed in vacuum, the urinary sample was chromatographed over a HP-20 macroporous resin column (5.0 × 120 cm) eluted with water, 30% EtOH-H_2O, 60% EtOH-H_2O and 95% EtOH-H_2O, successively. The 60% EtOH-H_2O eluate (C, 3.0 g) was subjected to a ODS column (3.0 × 35.0 cm), eluted with a EtOH-H_2O gradient solvent system (15%, 20%, 30% v/v) to give three fractions (C1-3). Fraction C3 (532 mg) was subjected to preparative HPLC with 30% ACN-H_2O (t_R = 35 min), then subfraction C3C (4.3 mg) was further purified by Sephadex LH-20 column (0.8 × 20.0 cm) eluted with EtOH to yield **M4** (0.5 mg). The 95% EtOH-H_2O eluate (D, 0.6 g) was subjected to a Sephadex LH-20 column (3.0 × 37.0 cm) and then further purified by preparative HPLC (30% ACN-H_2O, 8 mL/min) as the mobile phase to yield **M1** (132.1 mg, t_R = 85 min), **M2** (4.6 mg, t_R = 80 min) and **M3** (8.2 mg, t_R = 103 min).

The collected feces (490 g) were dried naturally, and then were extracted with EtOAc (1500 mL × 3). The extracts (31.2 g) of were successively separated by silica gel CC (5.5 × 70 cm, 200-300 mesh, 350 g), eluted with a cyclohexane-EtOAc (20:1, 10:1, 10:2, 10:3, 2:1, 1:1, 0:1, v/v) to yield 7 fractions (F1-7). Fraction F1 (651.3 mg) was isolated by preparative HPLC (80% ACN-H_2O, 3 mL/min) as the mobile phase to yield **M9** (0.6 mg, t_R = 25 min) and bakuchiol (98.2 mg, t_R = 27 min). Fraction F3 (1.9 g) was subjected to a

Sephadex LH-20 column (3.0 × 35.0 cm) and then further purified by preparative HPLC (52% ACN-H_2O, 3 mL/min) to yield **M5** (1.6 mg, t_R = 94 min), and **M6** (2.3 mg, t_R = 100 min). Fraction F4 (2.5 g) was also subjected to a Sephadex LH-20 column (3.0 × 37 cm) eluted with EtOH and preparative HPLC (49% ACN-H_2O, 8 mL/min) to afford **M7** (1.5 mg, t_R = 92 min), and **M8** (2.1 mg, t_R = 104 min). Fraction F5 (1.5 g) was separated by Sephadex LH-20 (3.0 × 35.0 cm) eluted with EtOH and preparative HPLC (78% ACN-H_2O, 8 mL/min) to afford **M11** (3.2 mg, t_R = 70 min) and **M10** (3.7 mg, t_R = 90 min). Fraction F6 (572.2 mg) was purified by preparative HPLC (79% ACN-H_2O, 3 mL/min) as the mobile phase to yield **M12** (3.9 mg, t_R = 30 min).

M1: white colorless oil; $[\alpha]_D^{25}$ + 27.6 (c 0.5 MeOH); UV (MeOH) λ_{max} (log ε): 205 (4.64), 262 (3.51) nm; IR (KBr) ν_{max}: 3426, 2926, 2861, 1727 cm^{-1}; ^1H and ^{13}C NMR data (see Table 1); HRESIMS *m*/*z* 245.1177 $[M-H]^-$ (Calcd for $C_{15}H_{17}O_3$, 245.1178).

M2: white colorless oil; $[\alpha]_D^{25}$ + 6.7 (c 0.5 MeOH); UV (MeOH) λ_{max} (log ε): 205 (4.34), 263 (3.30) nm; IR (KBr) ν_{max}: 3438, 2926, 2861, 1739 cm^{-1}; ^1H and ^{13}C NMR data (see Table 1); HRESIMS *m*/*z* 275.1288 $[M-H]^-$ (Calcd for $C_{16}H_{19}O_4$, 275.1283).

M3: colorless oil; $[\alpha]_D^{25}$ + 3.2 (c 0.75, MeOH); UV (MeOH) λ_{max} (log ε): 204 (4.28), 262 (3.51) nm; IR (KBr) ν_{max}: 3437, 2923, 1712 cm^{-1}; ^1H and ^{13}C NMR data (see Table 1 and 2); HRESIMS *m*/*z* 275.1288 $[M-H]^-$ (Calcd for $C_{16}H_{19}O_4$, 275.1283).

M4: colorless oil; $[\alpha]_D^{25}$ + 4.3 (c 0.2, MeOH); UV (MeOH) λ_{max} (log ε): 205 (4.67), 262 (3.82) nm; IR (KBr) ν_{max}: 3438, 2926, 2865, 1725 cm^{-1}; ^1H and ^{13}C NMR data (see Table 1); HRESIMS *m*/*z* 307.1541 $[M-H]^-$ (Calcd for $C_{17}H_{24}O_5$, 307.1545).

M5: colorless oil; $[\alpha]_D^{25}$ + 15.1 (c 0.5, MeOH); UV (MeOH) λ_{max} (log ε): 204 (4.29), 263 (1.92) nm; IR (KBr) ν_{max}: 3437, 2923, 2861, 1714 cm^{-1}; ^1H and ^{13}C NMR data (see Table 2); HRESIMS *m*/*z* 271.1704 $[M-H]^-$ (Calcd for $C_{18}H_{23}O_2$, 271.1698).

M6: colorless oil; $[\alpha]_D^{25}$ + 6.4 (c 0.3, MeOH); UV (MeOH) λ_{max} (log ε): 204 (4.05), 262 (2.26) nm; IR (KBr) ν_{max}: 3436, 2925, 2857, 1715 cm^{-1}; ^1H and ^{13}C NMR data (see Table 2); HRESIMS *m*/*z* 273.1850 $[M-H]^-$ (Calcd for $C_{18}H_{25}O_2$, 273.1855).

M7: colorless oil; $[\alpha]_D^{25}$ +4.2 (c 0.2, MeOH); UV (MeOH) λ_{max} (log ε): 204 (4.19), 261 (1.89) nm; IR (KBr) ν_{max}: 3439, 2926, 2866, 2358, 1715 cm^{-1}; ^1H and ^{13}C NMR data (see Table 2); HRESIMS *m*/*z* 285.1493 $[M-H]^-$ (Calcd for $C_{18}H_{21}O_3$, 285.1491).

M8: colorless oil; $[\alpha]_D^{25}$ + 4.3 (c 0.25, MeOH); UV (MeOH) λ_{max} (log ε): 204 (4.59), 262 (3.05) nm; IR (KBr) ν_{max}: 3439, 2931, 2861, 1748 cm^{-1}; ^1H and ^{13}C NMR data (see Table 2); HRESIMS *m*/*z* 287.1651 $[M-H]^-$ (Calcd for $C_{18}H_{23}O_3$, 287.1647).

M9: colorless oil; $[\alpha]_D^{25}$ + 16.1 (c 0.2, MeOH); UV (MeOH) λ_{max} (log ε): 205 (4.45), 263 (2.83) nm; IR (KBr) ν_{max}: 3427, 2929, 2861, 1716 cm^{-1}; ^1H and ^{13}C NMR data (see Table 2); HRESIMS *m*/*z* 255.1754 $[M-H]^-$ (Calcd for $C_{18}H_{23}O$, 255.1749).

M10: colorless oil; $[\alpha]_D^{25}$ + 27.5 (c 1.0, MeOH); UV (MeOH) λ_{max} (log ε): 205 (4.49), 263 (3.52) nm; IR (KBr) ν_{max}: 3438, 2935, 2870, 1709 cm^{-1}; ^1H and ^{13}C NMR data (see Table 3); HRESIMS *m*/*z* 619.3994 $[M-H]^-$ (Calcd for $C_{39}H_{55}O_6$, 619.3999).

M11: colorless oil; $[\alpha]_D^{25}$ + 21.5 (c 0.75, MeOH); UV (MeOH) λ_{max} (log ε): 204 (4.36), 263 (2.37) nm; IR (KBr) ν_{max}: 3438, 2928, 2866, 1710 cm^{-1}; ^1H and ^{13}C NMR data (see Table 3); HRESIMS *m*/*z* 619.3992 $[M-H]^-$ (Calcd for $C_{39}H_{55}O_6$, 619.3999).

M12: colorless oil; $[\alpha]_D^{25}$ + 17.5 (c 1.0, MeOH); UV (MeOH) λ_{max} (log ε): 204 (4.69), 263 (3.32) nm; IR (KBr) ν_{max}: 3427, 2929, 2870, 1709 cm^{-1}; ^1H and ^{13}C NMR data (see Table 3); HRESIMS *m*/*z* 635.3951 $[M-H]^-$ (Calcd for $C_{39}H_{55}O_7$, 635.3948).

*2.4. Absolute configuration of the 1,2-diol moiety in **M4***

According to the published procedure [13], a mixture of 1:1.2 diol/$Mo_2(OAc)_4$ for **M4** was subjected to CD measurement at a concentration of 1 mg/mL. The first CD spectrum was recorded immediately after mixing, and its time evolution was monitored until stationary (about 10 min after mixing). The inherent CD was subtracted. The observed sign of the diagnostic bands at around 310 nm in the induced CD spectrum was correlated to the absolute configuration of the 1,2-diol moiety.

2.5. MC3T3-E1 activities and HKC-8 cytotoxicity assay

2.5.1 Cell culture

MC3T3-E1 cells (murine pre-osteoblastic cell line, ATCC no.CRL-1661) and HKC-8 cells (human renal proximal tubular cell line) were routinely cultured in Minimum essential medium alpha (MEMα) and Dulbecco's modified eagle medium (DMEM)/F12 medium, respectively, supplemented with 10% fetal bovine serum (FBS), penicillin 100 U/mL and streptomycin 100 μg/mL at 37 °C in a humidified atmosphere of 95% air and 5% CO_2. Cells were trypsinized with 0.05% trypsin-EDTA (Gibico, USA) and were cultured in a new culture plate at 80% confluence.

2.5.2 Alkaline phosphatase (ALP) activity assay

The ALP activity of MC3T3-E1 cells were measured by Wako lab assay ALP kit

(Wako, Japan). MC3T3-E3 cells were seeded in 96 plates at a cell density of 1.2×10^4 cells per well. After 48h, cells were treated with bakuchiol (10^{-9} M to 10^{-5} M), **M1**-**M3** (10^{-9} M to 10^{-5} M), 17β-estradiol (E2) or vehicle (1% ethanol) in the presence of ascorbic acid (50 μg/ml) and β-glycerophosphate (10 mM) for 7 days. After treatment, the medium was removed, the cells were washed twice with PBS and 100 μL/well PLB (Passive Lysis Buffer, Promega, lot000106412) was added to each well. After shaking for 15 min, 20 μL lysed solution was transferred to a new 96 well plate with 100 μL/well p-NPP (p-Nitrpphenylphophate Disodium 6.7 mmol/L) and incubated at 37 °C for 15 minutes. Finally, the absorbance was measured at 405 nm by a microplate reader (Bio-Rad Laboratories Inc., USA) and ALP activity was normalised by the protein content of the whole wells which was also detected by at 595 nm by using Bradford protein assay.

2.5.3 Cell cytotoxic effect assay by MTS

The cell viability was detection by MTS assay. HKC-8 cells were seeded in 96 plates at a cell density of 5×10^3 cells/well. After 24h, cells were treating with bakuchiol 5 μM to 50 μM, **M1**-**M3** (5 μM to 50 μM) or negative control including Blank and vehicle (1% ethanol) groups for 24 h, the medium was discarded and replaced with 100 μL MTS/PMS solution (Promega, Madison, WI, USA). After incubation at 37 °C for 1 h, the absorbance at 490 nm was measured on a microplate reader (Bio-Rad Laboratories Inc., USA).

2.5.5 Statistical analysis

All results were presented as mean ± SEM of three independent experiments, each in triplicate or more. Differences were analyzed statistically with varience (one way ANOVA)

and Tukey's HSD test between control group and each treatment group by using The Graph-Pad Prism version 5.01 software. $P < 0.05$ was considered as significant.

3. Result and discussion

Twelve metabolites were isolated from rat's urine and feces after oral administration of bakuchiol by using various chromatographic methods. Among them, **M2** to **M12** were new compounds. All the structures were identified based on MS and NMR data analysis.

The ^{1}H and ^{13}C NMR spectra (Table 1) of **M1** were in agreement with those reported [15] for norbakuchinic acid. However, there were two incorrect assignments in the literature. In the HSQC spectrum, the methylene protons at δ_H 1.71 (H-10) corresponded to carbon resonance at δ_C 35.4 (C-10), and the methylene protons at δ_H 2.15 (H-11) corresponded to carbon resonance at δ_C 29.5 (C-11), which indicated that these proton signals were confusion in the literature.

The molecular formula of **M2** was determined to be $C_{16}H_{20}O_4$ on the basis of HRESIMS. The ^{13}C NMR of **M2** spectrum displayed 16 signals and showed similarities to that of **M1** except for the 1,4-disubstituted benzene moiety. Comprehensive analysis of NMR spectroscopic data of **M2** indicated that **M2** was the methoxylation product of **M1**. The HMBC correlations of δ_H 3.91/δ_C 146.8 (C-3), δ_H 6.88 (H-2)/δ_C 145.3 (C-4), and δ_H 6.86 (H-6)/δ_C 145.3 (C-4) suggested that the methoxy group was located at C-3. Thus, **M2** was elucidated as 3-methoxynorbakuchinic acid.

M3 had the same molecular formula as **M2**. The key HMBC correlations of δ_H 3.88/δ_C 146.2 (C-4), δ_H 6.99 (H-2)/δ_C 146.2 (C-4), and δ_H 6.82 (H-6)/δ_C 146.2 (C-4) suggested that the methoxy group was located at C-4. Accordingly, **M3** was identified as

3-hydroxy-4-methoxynorbakuchinic acid.

The molecular formula of **M4** was established as $C_{17}H_{24}O_5$ by HRESIMS. The NMR data of M4 (Table 1) was similar to those of M1, except for the terminal olefin moiety. The typical oxygenated methane carbon signals at δ 78.0 (C-17), δ 62.8 (C-18) and HMBC correlations from H-17 (δ 3.25) to C-8 (δ 131.8)/C-10 (δ 32.2)/C-16 (δ 19.2), and from H-18 (δ 3.49 and 3.18) to C-17 (δ 78.0) suggested that the terminal olefin of M1 was replaced by a 1,2-diol moiety of M4 (Fig. 2) and the two hydroxyl groups were located at C-17 and C-18, respectively. The absolute configuration of the 1,2-diol moiety in **M4** was assigned using the in situ dimolybdenum CD method, developed by Snatzke and Frelek [16]. The positive cotton effect at around 310 nm, observed in the induced CD spectrum, permitted the assignment of absolute configuration to be 17S on the basis of the empirical rule proposed by Snatzke (Fig. 2). Consequently, **M4** was assigned as (17S)-17,18-dihydroxynorbakuchinic acid ethyl ester.

The molecular formula of **M5** was determined to be $C_{18}H_{24}O_2$ ($[M-H]^-$ *m/z* 271.1704), 16 Da more than bakuchiol. NMR spectroscopic data (Table 2) suggested that **M5** was the oxylation product of bakuchiol [17], which was confirmed by an obvious downfield shift from δ_C 17.7 to 61.6 at C-14 position. Thus, **M5** was confirmed as 14-hydroxy-bakuchiol. The molecular formula of **M6** was established as $C_{18}H_{26}O_2$ ($[M-H]^-$ *m/z* 273.1850), 2 Da more than **M5**. In the ^{13}C NMR spectrum, the obvious upfield shift of C-12 (δ 128.8 to 34.0) and C-13 (δ 134.1 to 35.8) suggested that the 12(13)-double bond in **M5** was hydrogenised in **M6**. Thus, **M6** was identified as 12,13-dihydrogen-14-hydroxy-bakuchiol.

The molecular formula of **M7** was deduced to be $C_{18}H_{22}O_3$ on the basis of HRESIMS.

The NMR spectra of **M7** had considerable resemblance to those of bakuchiol(Table 2), except that an additional carboxyl group (δ_C 171.9) replaced a methyl group (δ_C 25.7, C-15). It indicated that M7 was 15-carboxylbakuchiol. The disappearance of NOESY correlation between CH_3-15 and H-12 further proved this elucidation. The molecular formula of **M8** was determined to be $C_{18}H_{24}O_3$, 2 Da more than **M7**. Comprehensive NMR data analysis demonstrated that **M8** was 12,13-dihydrogen-15-carboxylbakuchiol.

The molecular formula of **M9** was determined to be $C_{18}H_{24}O$ according to the HRESIMS. The 1D NMR data (Table 2) were similar to those of 12-hydroxyisobakuchiol [17], except the absence of hydroxyl group in C-12, which was confirmed by an obvious upfield shift from δ_C 77.7 to 38.5. Therefore, **M9** was assigned as isobakuchiol.

The molecular formula of **M10** was deduced to be $C_{39}H_{56}O_6$ according to the HRESIMS. The ^1H and ^{13}C NMR spectra (Table 3) showed the characteristic signals for a norbakuchinic acid moiety. Moreover, there were 24 additional signals, consisting of three methyls, ten methylenes, eight methines (including two oxygenated methines), as well as three quaternary carbons (including one carbonyl), which indicated **M10** has a bile acid moiety. By comparing with literature [18], the NMR signals of bile acid moiety were similar with those of chenodeoxycholic acid. The key HMBC correlations from H-3′ (δ 4.55) to C-12 (δ 174.0) (Fig. 3), indicated the linkage between these two moieties. Since 3α-bile acids were the mainly existing form in vertebrate [19], the structure of **M10** was elucidated as shown in Fig.3. Similarly, by comparison with literatures [18,20] and combined with 1D and 2D NMR data analysis, the structures of **M11** and **M12** were elucidated as shown in Fig.4.

Since bone alkaline phosphatase is a traditional marker of bone turnover, and it was reported that bakuchiol could reduce postmenopausal bone loss by increasing alkaline phosphatase (ALP) [7], the ALP activity on MC3T3-E1 cells of bakuchiol and three main metabolites M1-M3 were evaluated. Upon treatment for 2 days, bakuchiol (10^{-9} M to 10^{-5} M) could induce a dose-dependent increasing on ALP activity (Fig.5), while for its metabolites, only **M1** and **M2** showed weak increasing on ALP activity at the highest concentration (10^{-5} M). It was report that bakuchiol had kidney toxicity [9], so the cytotoxicity against HKC-8 cells were also evaluated. As shown in Fig. 6, bakuchiol exerted a dose-dependent cytotoxic activity on HKC-8 cells from 12.5 μM to 50 μM, while metabolites **M1**-**M3** showed no cytotoxicity even at the highest concentration 50 μM. In conclusion, bakuchiol not only showed noteworthy ALP activity on MC3T3-E1 cells, but also exhibited cytotoxicity on HKC-8 cells, which might account for the renal toxicity of *Psoralea corylifolia* on human body. However, its metabolites showed no cytotoxicity at test concentration. These results suggested that *in vivo* metabolism reduced the toxicity of bakuchiol, which might be a detoxification process.

In this work, 12 metabolites, including 11 new compounds, were isolated from the urine and feces of rats after oral administration of bakuchiol. The chemical structure of these metabolites were elucidated by comprehensive analysis of NMR data. It demonstrated that bakuchiol could undertake oxidation (**M1**, **M4**, **M5** and **M7**), reduction (**M6**, **M8**), methylation (**M2**, **M3**), isomerization (**M9**) and bile acid conjugation (**M10**, **M11** and **M12**) reactions in rats. In addition, the possible metabolic pathways of bakuchiol *in vivo* are also proposed as shown in Fig. 4.

In the previous study [12], we characterized the metabolites of bakuchiol by UPLC/Q-TOF-MS. In this paper, through the chemical separation and NMR data analysis, the chemical structures of these metabolites were ambitiously identified, and the activity of some metabolites were also evaluated. Furthermore, a rare metabolic reaction, bile acid conjugation reaction (**M10**, **M11** and **M12**), was discovered. Bile acids, synthesized in liver, are involved in a number of metabolic processes and play a critical role in lipid digestion and cholesterol metabolism. They could undergo 7α-dehydroxylation, deconjugation, and oxidation/epimerization of hydroxyl groups at C-3, C-7 and C-12 in human colon, or suffer sulfation and glucuronidation at C-24 in the liver [21,22]. However, there was no literature reported that bile acids could be biotransformed with xenobiotics at C-3 position *in vivo*. By far as our best knowledge, the bile acid conjugation with xenobiotics at C-3 position *in vivo* was discovered for the first time.

Conflict of interest

The authors declare no conflict of interest.

Acknowledgement

We thank Liu-yuan Chen, Wen-jing Tian, Zi-fei Qin and Xiu-yu Shen for measuring the NMR and HRESIMS data. This work was supported by National Natural Science Foundation of China Research Grant Council (81220108028) and the Programme of Introducing Talents of Discipline to Universities (B13038).

Appendix A. Supplementary data

The HRESI-MS, 1D NMR and 2D NMR for **M1**-**M12** are available in

Supplementary data. Supplementary data associated with this article can be found online at

References

[1] The Pharmacopoeia Commission of People's Republic of China, Pharmacopoeia of the People's Republic of China, 2010 ed., Chemical Industry Press, Beijing, 2010; 174.

[2] Chen Z, Jin K, Gao LY, Lou GD, Jin Y, Yu YP, et al. Anti-tumor effects of bakuchiol, an analogue of resveratrol, on human lung adenocarcinoma A549 cell line. Eur J Pharmacol 2010; 643: 170-179.

[3] Katsura H, Tsukiyama RI, Suzuki A, Kobayashi M. In vitro antimicrobial activities of bakuchiol against oral microorganisms. Antimicrob Agents Chemother 2001; 45: 3009-3013.

[4] Pae HO, Cho H, Oh GS, Kim NY, Song EK, Kim YC, et al. Bakuchiol from *Psoralea corylifolia* inhibits the expression of inducible nitric oxide synthase gene via the inactivation of nuclear transcription factor-*κ*B in RAW 264.7 macrophages. Int Immunopharmacol 2001; 1: 1849-1855.

[5] Backhouse CN, Delporte CL, Negrete RE, Erazo S, Zuñiga A, Pinto A, et al. Active constituents isolated from *Psoralea glandulosa* L. with antiinflammatory and antipyretic activities. J Ethnopharmacol 2001; 78: 27-31.

[6] Choi SY, Lee S, Choi WH, Lee Y, Jo YO, Ha TY. Isolation and anti-inflammatory activity of bakuchiol from *Ulmus davidiana* var. *japonica*. J Med Food 2010; 13: 1019-1023.

[7] Lim SH, Ha TY, Kim SR, Ahn J, Park HJ, Kim S. Ethanol extract of *Psoralea corylifolia* L. and its main constituent, bakuchiol, reduce bone loss in ovariectomised

Sprague–Dawley rats. Brit J Nutr 2009; 101: 1031-1039.

[8] Lim SH, Ha TY, Ahn J, Kim S. Estrogenic activities of *Psoralea corylifolia* L. seed extracts and main constituents. Phytomedicine 2011; 18: 425-430.

[9] Jiang F, Zhou XR, Wang Q, Zhang BX. Cytotoxic effect and mechanism of bakuchiol and bakuchiol combined with psoralen on HK-2 cell. Chin J Pharmacol Toxicol 2010; 1: 50-58.

[10] Zhuang XM, Zhong YH, Yuan M, Li H. Pre-column derivatization combined with UHPLC-MS/MS for rapid and sensitive quantification of bakuchiol in rat plasma. J Pharm Biomed Anal 2013; 75: 18-24.

[11] Zhang SQ, Fan YM. Ultra-high-performance liquid chromatography-tandem mass spectrometry for pharmacokinetics of bakuchiol in rats. Biomed Chromatogr 2014; 28: 433-438.

[12]Wang PL, Yao ZH, Zhang FX, Shen XY, Dai Y, Qin L, et al. Identification of metabolites of PSORALEAE FRUCTUS in rats by ultra performance liquid chromatography coupled with quadrupole time-of-flight tandem mass spectrometry analysis. J Pharm Biomed Anal 2015; 112: 23-35.

[13] Jia CQ, Shi HM, Jin W, Zhang K, Jiang Y, Zhao MB, et al. Metabolism of echinacoside, a good antioxidant, in rats: isolation and identification of its biliary metabolites. Drug Metab Dispos 2009; 37: 431-438.

[14] Lou Y, Zhang H, He H, Peng KF, Kang N, Wei XC, et al. Isolation and identification of phase 1 metabolites of curcumol in rats. Drug Metab Dispos 2010; 38: 2014-2022.

[15] Ryu SY, Choi SU, Lee CO, Zee OP. Antitumor activity of *Psoralea corylifolia*. Arch

Pharm Res 1992; 15: 356-359.

[16] Di Bari L, Pescitelli G, Pratelli C, Pini D, Salvadori P. Determination of absolute configuration of acyclic 1,2-diols with $Mo_2(OAc)_4$. 1. Snatzke's method revisited. J Org Chem 2001; 66: 4819-4825.

[17] Labbé C, Faini F, Coll J, Connolly JD. Bakuchiol derivatives from the leaves of *Psoralea glandulosa*. Phytochemistry 1996; 42: 1299-1303.

[18] Waterhous DV, Barnes S, Muccio DD. Nuclear magnetic resonance spectroscopy of bile acids. Development of two-dimensional NMR methods for the elucidation of proton resonance assignments for five common hydroxylated bile acids, and their parent bile acid, 5β-cholanoic acid. J Lipid Res 1985; 26: 1068-1078.

[19] Mukhopadhyay S, Maitra U. Chemistry and biology of bile acids. Curr Sci India 2004; 87: 1666-1683.

[20] Davis DG, Thompson MB. Nuclear magnetic resonance identification of the taurine conjugate of 3α,6β,7β-trihydroxy-5β,22-cholen-24-oic acid (tauro-Δ^{22}-β-muricholate) in the serum of female rats treated with α-naphthyilsothiocyanate. J Lipid Res 1993; 34: 651-661.

[21] Monte MJ, Marin JJG, Antelo A, Vazquez-Tato J. Bile acids: chemistry, physiology, and pathophysiology. World J Gastroenterol 2009; 15: 804-816.

[22] Lefebvre P, Cariou B, Lien F, Kuipers F, Staels B. Role of bile acids and bile acid receptors in metabolic regulation. Physiol Rev 2009; 89: 147-191.

Legend to figures

Fig. 1. The chemical structure of bakuchiol.

Fig. 2. Key HMBC (→) correlations and CD spectrum of **M4**.

Fig. 3. Key HMBC (→) correlations of **M10**.

Fig. 4. Proposed metabolic pathway of bakuchiol.

Fig. 5. Effects of bakuchiol and M1-M3 on ALP activity in MC3T3-E1 cells. Each value is the mean ± SEM of three independent experiments, each in triplicate. *p < 0.05 and **p < 0.01, ***P < 0.001 compared with the control group that with vehicle ethanol.

Fig. 6. Effects of bakuchiol and M1-M3 on cytotoxicity in HKC-8 cells. Each value is the mean ± SEM of three independent experiments, each in 9 wells. *p < 0.05 and **p < 0.01, ***P < 0.001 compared with the control group that with vehicle ethanol.

Table 1 1D NMR data for M1-M4 (M1-M3 were measured in $CDCl_3$, and M4 was measured in DMSO-d_6).

Table 2 1D NMR data for M5-M9 (Measured in $CDCl_3$, 600 MHz for ^1H).

Table 3 1D NMR data for M10-M12 (M10-M11 were measured in $CDCl_3$; M12 was measured in DMSO-d_6; 600 MHz for ^1H).

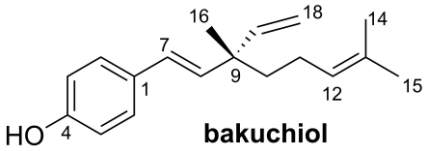

Fig. 1. The chemical structure of bakuchiol.

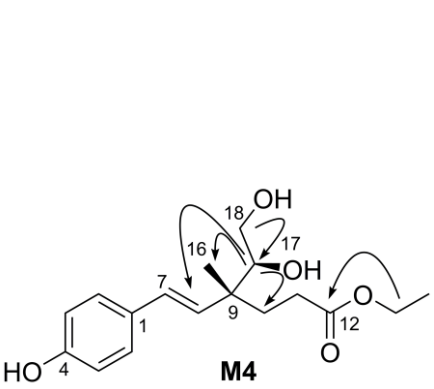

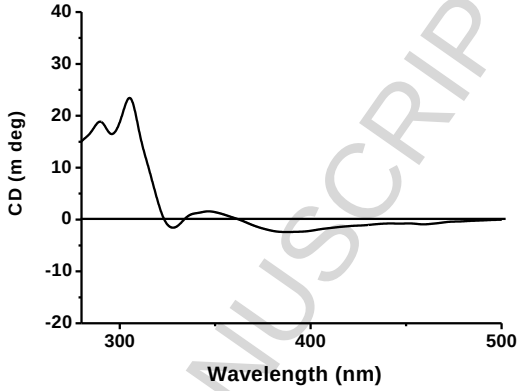

Fig. 2. Key HMBC (→) correlations and CD spectrum of **M4**.

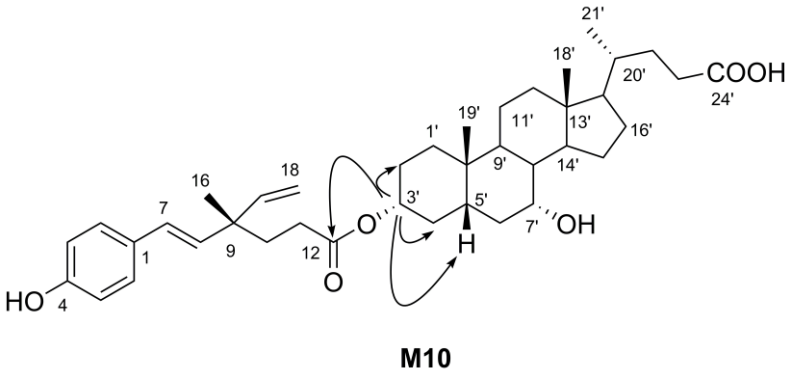

Fig. 3. Key HMBC (→) correlations of **M10**.

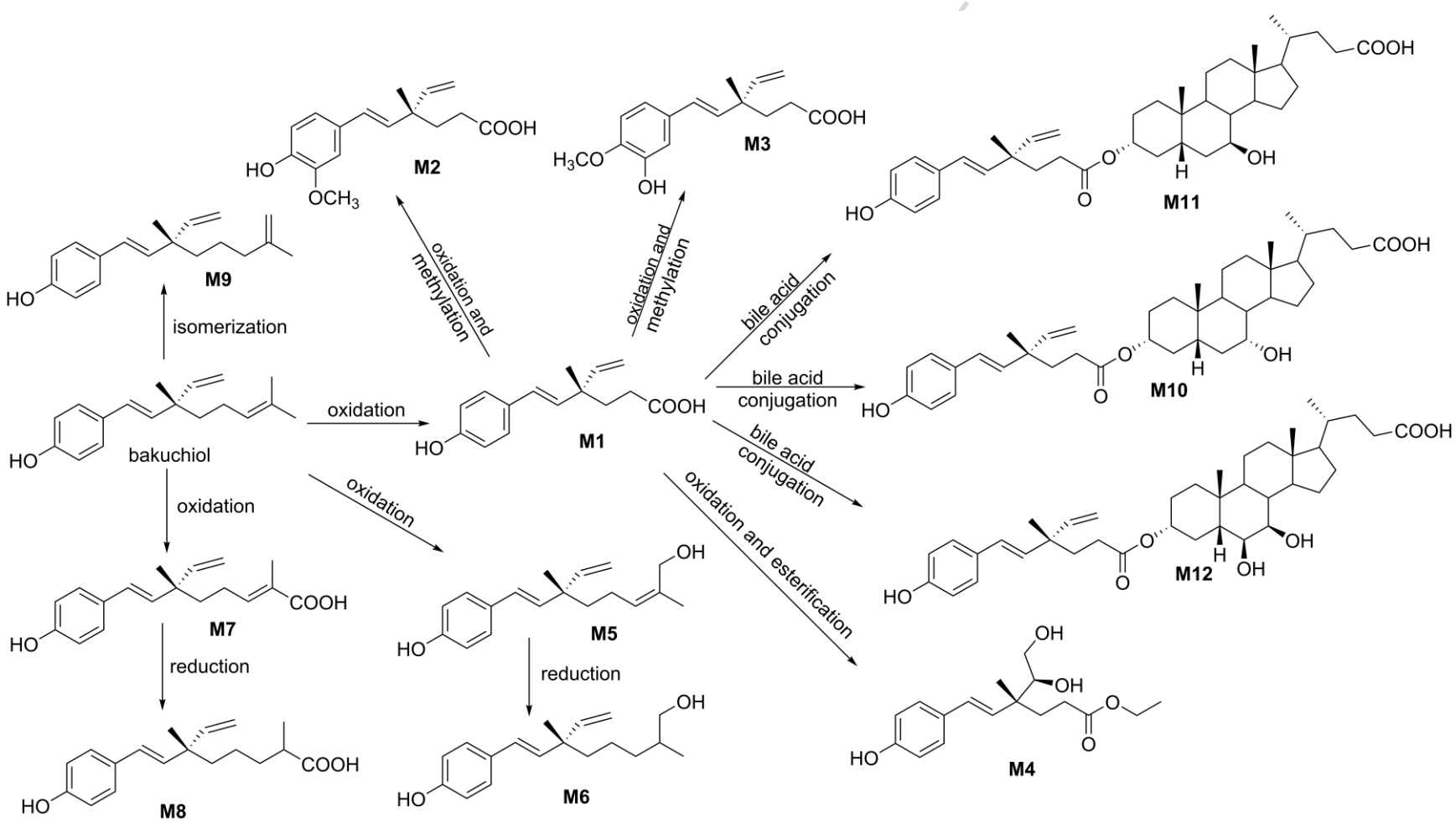

Fig. 4. Proposed metabolic pathway of bakuchiol.

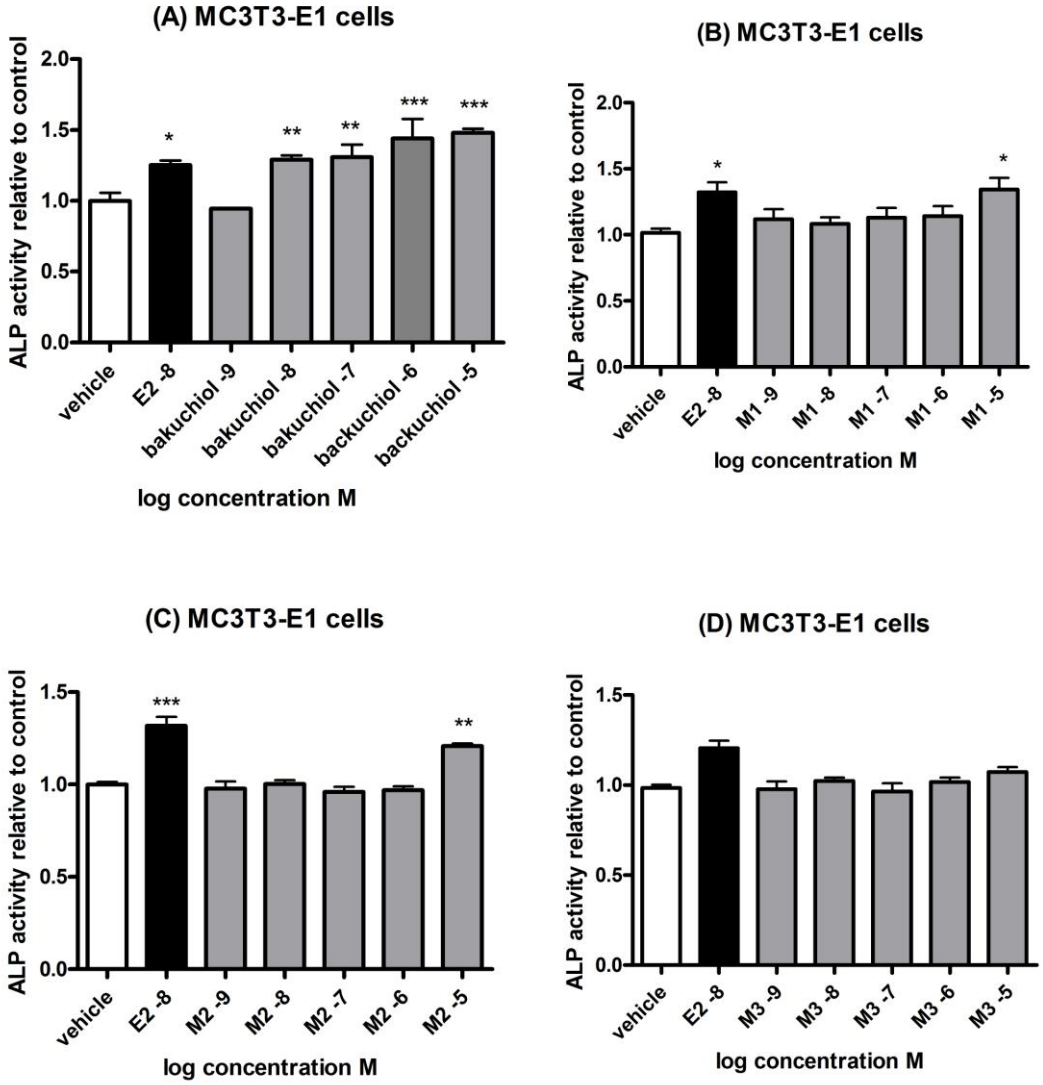

Fig. 5. Effects of bakuchiol and M1-M3 on ALP activity in MC3T3-E1 cells. Each value is the mean ± SEM of three independent experiments, each in triplicate. *p < 0.05 and **p < 0.01, ***P < 0.001 compared with the control group that with vehicle ethanol.

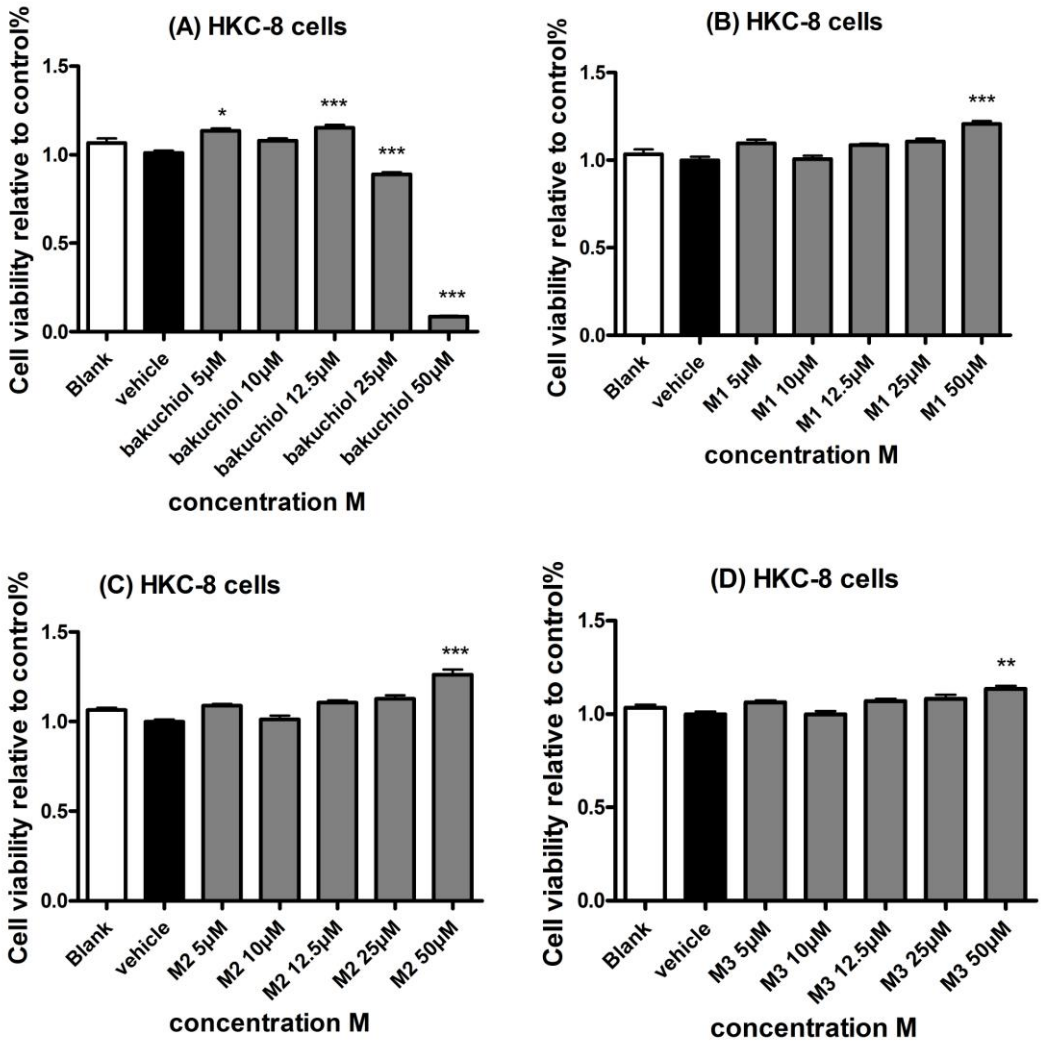

Fig. 6. Effects of bakuchiol and M1-M3 on cytotoxicity in HKC-8 cells. Each value is the mean ± SEM of three independent experiments, each in 9 wells. *p < 0.05 and **p < 0.01, ***P < 0.001 compared with the control group that with vehicle ethanol.

Table 1 1D NMR data for **M1**-**M4** (**M1**-**M3** were measured in $CDCl_3$, and **M4** was measured in DMSO-d_6).

Position	**Norbakuchinic acid (M1)**[a]		**M2**[a]		**M3**[a]		**M4**[b]	
	δ_H (*J* in Hz)	δ_C	δ_H (*J* in Hz)	δ_C	δ_H (*J* in Hz)	δ_C	δ_H (*J* in Hz)	δ_C
1		128.2		130.2		131.5		128.5
2	7.22 (1H, d, 8.4)	127.2	6.88 (1H, overlapped)	108.3	6.99 (1H, brs)	111.8	7.18 (1H, d, 8.6)	127.1
3	6.69 (1H, d, 8.4)	115.3		146.8		145.9	6.69 (1H, d, 8.6)	115.3
4		156.7		145.3		146.2		156.5
5	6.69 (1H, d, 8.4)	115.3	6.85 (1H, overlapped)	114.6	6.78 (1H, d, 8.0)	110.8	6.69 (1H, d, 8.6)	115.3
6	7.22 (1H, d, 8.4)	127.2	6.86 (1H, overlapped)	119.9	6.82 (1H, brd, 8.0)	118.8	7.18 (1H, d, 8.6)	127.1
7	6.20 (1H, d, 16.3)	126.9	6.26 (1H, d, 16.3)	128.1	6.24 (1H, d, 16.2)	127.8	6.16 (1H, d, 16.5)	127.5
8	6.01 (1H, d, 16.3)	133.4	5.99 (1H, d, 16.3)	134.4	6.00 (1H, d, 16.2)	135.1	6.03 (1H, d, 16.5)	131.8
9		41.6		42.2		42.2		42.1
10	1.71 (2H, t, 7.8)	35.4	1.87 (2H, t, 8.2)	35.4	1.85 (2H, t, 8.2)	35.4	1.79 (1H, m) 1.68 (1H, m)	32.2
11	2.15 (2H, t, 7.8)	29.5	2.35 (2H, t, 8.2)	29.4	2.34 (2H, t, 8.2)	29.5	2.23 (1H, m) 2.12 (1H, m)	39.0
12		174.7		178.0		178.1		173.4
16	1.12 (3H, s)	22.9	1.21 (3H, s)	23.5	1.19 (3H, s)	23.5	0.99 (3H, s)	19.2
17	5.86 (1H, dd, 17.5, 10.8)	145.4	5.85 (1H, dd, 17.4, 10.8)	145.0	5.84 (1H, dd, 17.6, 10.8)	144.9	3.25 (1H, m)	78.0
18	5.00 (1H, d, 17.5) 5.03 (1H, d, 10.8)	112.2	5.06 (1H, d, 17.4) 5.09 (1H, d, 10.8)	113.1	5.04 (1H, d, 17.6) 5.08 (1H, d, 10.8)	113.1	3.49 (1H, m) 3.18 (1H, m)	62.8
3-OCH_3			3.91 (3H, s)	56.1				
4-OCH_3					3.88 (3H, s)	56.2		
4-OH							9.38 (1H, brs)	
17-OH							4.63 (1H, d, 4.7)	
18-OH							4.35 (1H, brs)	
-CH_2CH_3							3.98 (2H, m) 1.12 (3H, t, 7.1)	59.6 14.0

[a] Recorded at 400 MHz for ^1H.
[b] Recorded at 600 MHz for ^1H.

Table 2 1D NMR data for **M5**-**M9** (Measured in $CDCl_3$, 600 MHz for ^1H).

Position	**M5**		**M6**		**M7**		**M8**		**M9**	
	δ_H (*J* in Hz)	δ_C	δ_H (*J* in Hz)	δ_C	δ_H (*J* in Hz)	δ_C	δ_H (*J* in Hz)	δ_C	δ_H (*J* in Hz)	δ_C
1		130.7		131.0		130.7		130.9		131.1
2	7.24 (1H, d, 8.5)	127.4	7.25 (1H, d, 8.5)	127.5	7.25 (1H, d, 8.5)	127.6	7.24 (1H, d, 8.5)	127.5	7.25 (1H, d, 8.6)	127.5
3	6.77 (1H, d, 8.5)	115.4	6.77 (1H, d, 8.5)	115.5	6.77 (1H, d, 8.5)	115.6	6.76 (1H, d, 8.5)	115.5	6.77 (1H, d, 8.6)	115.5
4		154.8		154.9		155.0		154.9		154.8
5	6.77 (1H, d, 8.5)	115.4	6.77 (1H, d, 8.5)	115.5	6.77 (1H, d, 8.5)	115.6	6.76 (1H, d, 8.5)	115.5	6.77 (1H, d, 8.6)	115.5
6	7.24 (1H, d, 8.5)	127.4	7.25 (1H, d, 8.5)	127.5	7.25 (1H, d, 8.5)	127.6	7.24 (1H, d, 8.5)	127.5	7.25 (1H, d, 8.6)	127.5
7	6.25 (1H, d, 16.3)	126.7	6.24 (1H, d, 16.2)	126.6	6.27 (1H, d, 16.2)	127.3	6.23 (1H, d, 16.3)	126.7	6.24 (1H, d, 16.2)	126.6
8	6.03 (1H, d, 16.3)	135.5	6.04 (1H, d, 16.2)	136.1	6.03 (1H, d, 16.2)	135.1	6.02 (1H, d, 16.3)	135.9	6.05 (1H, d, 16.2)	136.2
9		42.5		42.7		42.6		42.6		42.6
10	1.51 (2H, t, 7.1)	41.6	1.46 (2H, m)	41.7	1.62 (2H, t, 7.4)	39.7	1.47 (2H, m)	41.2	1.45 (2H, m)	41.0
11	2.03 (2H, m)	22.9	1.26 (2H, m)	21.9	2.17 (2H, t, m)	24.5	1.32 (2H, m)	22.2	1.43 (2H, m)	22.5
12	5.30 (1H, t, 7.1)	128.8	1.37 (1H, m) 1.09 (1H, m)	34.0	6.89 (1H, t, 7.4)	145.3	1.68 (1H, m) 1.40 (1H, m)	34.3	2.00 (2H, t, 7.1)	38.5
13		134.1	1.62 (m)	35.8		126.8	2.47 (m)	39.1		146.0
14	4.11 (2H, s)	61.6	3.41 (1H, dd, 10.4, 6.4) 3.50 (1H, dd, 10.4, 5.8)	68.5	1.81 (3H, s)	12.2	1.16 (3H, d, 6.7)	17.1	4.69 (1H, s) 4.66 (1H, s)	110.1
15	1.78 (3H, s)	21.2	0.90 (3H, d, 6.7)	16.7		171.9		181.2	1.69 (3H, s)	22.5
16	1.19 (3H, s)	23.4	1.18 (3H, s)	23.6	1.22 (3H, s)	23.6	1.17 (3H, s)	23.6	1.18 (3H, s)	23.6
17	5.86 (1H, dd, 17.5, 10.7)	145.7	5.87 (1H, dd, 17.4, 10.8)	146.3	5.87 (1H, dd, 17.5, 10.7)	145.4	5.85 (1H, dd, 17.4, 10.8)	146.0	5.87 (1H, dd, 17.5, 10.7)	146.2
18	5.03 (1H, d, 10.7) 5.01 (1H, d, 17.5)	112.1	5.03 (1H, d, 10.8) 5.00 (1H, d, 17.4)	112.0	5.08 (1H, d, 10.7) 5.04 (1H, d, 17.5)	112.7	5.02 (1H, d, 10.8) 4.99 (1H, d, 17.4)	112.1	5.03 (1H, d, 10.7) 5.00 (1H, d, 17.5)	112.0

Table 3 1D NMR data for **M10**-**M12** (**M10**-**M11** were measured in $CDCl_3$; **M12** was measured in DMSO-d_6; 600 MHz for ^1H).

Position	**M10**		**M11**		**M12**	
	δ_H (*J* in Hz)	δ_C	δ_H (*J* in Hz)	δ_C	δ_H (*J* in Hz)	δ_C
1		130.5		130.6		128.1
2	7.23 (1H, d, 8.6)	127.6	7.24 (1H, d, 8.5)	127.6	7.21 (1H, d, 8.5 Hz)	127.2
3	6.76 (1H, d, 8.6)	115.6	6.77 (1H, d, 8.5)	115.8	6.69 (1H, d, 8.5 Hz)	115.3
4		155.2		155.2		156.8
5	6.76 (1H, d, 8.6)	115.6	6.77 (1H, d, 8.5)	115.8	6.69 (1H, d, 8.5 Hz)	115.3
6	7.23 (1H, d, 8.6)	127.6	7.24 (1H, d, 8.5)	127.6	7.21 (1H, d, 8.5 Hz)	127.2
7	6.25 (1H, d, 16.2)	127.4	6.25 (1H, d, 16.2)	127.5	6.19 (1H, d, 16.3)	127.0
8	5.99 (1H, d, 16.2)	134.7	5.99 (1H, d, 16.2)	134.6	5.99 (1H, d, 16.3)	133.0
9		42.2		42.4		41.7
10	1.81 (2H, m)	35.8	1.84 (2H, m)	35.4	1.73 (2H, m)	35.3
11	2.25 (2H, m)	30.6	2.26 (2H, t, 7.8)	30.4	2.19 (2H, t, 7.8)	29.7
12		174.0		173.7		172.5
16	1.17 (3H, s)	23.5	1.19 (3H, s)	24.1	1.12 (3H, s)	22.8
17	5.84 (1H, dd, 17.5, 10.7)	145.2	5.84 (1H, dd, 17.7, 10.8)	145.0	5.86 (1H, dd, 17.6, 10.7)	145.3
18	5.03 (1H, d, 17.5) 5.06 (1H, d, 10.7)	112.8	5.03 (1H, d, 17.7) 5.07 (1H, d, 10.8)	112.9	5.00 (1H, d, 17.6) 5.03 (1H, d, 10.7)	112.3
1′	1.82 (1H, m) 1.01 (1H, m)	35.1	1.78 (1H, m) 1.05 (1H, m)	34.8	1.92 (1H, m) 1.12 (1H, m)	34.9
2′	1.63 (1H, m) 1.41 (1H, m)	26.9	1.62 (1H, m) 1.33 (1H, m)	26.6	1.49 (1H, m) 1.21 (1H, m)	25.8
3′	4.55 (1H, m)	74.5	4.60 (1H, m)	73.9	4.49 (1H, m)	73.1
4′	2.25 (1H, m) 1.68 (1H, m)	35.4	1.65 (1H, m) 1.55 (1H, m)	33.2	1.55 (1H, m) 1.39 (1H, m)	31.2
5′	1.42 (1H, m)	41.3	1.42 (1H, m)	42.4	1.64 (1H, m)	47.2
6′	1.96 (1H, m) 1.47 (1H, m)	34.5	1.77 (1H, m) 1.59 (1H, m)	36.6	3.38 (1H, brs)	74.7
7′	3.85 (1H, m)	68.7	3.49 (1H, m)	71.6	3.26 (1H, dd, 10.0, 3.4)	72.0
8′	1.48 (1H, m)	39.5	1.42 (1H, m)	42.4	1.58 (1H, m)	38.0
9′	1.82 (1H, m)	33.0	1.42 (1H, m)	39.4	1.34 (1H, m)	39.0
10′		35.2		34.2		33.5
11′	1.46 (1H, m) 1.26 (1H, m)	20.7	1.41 (1H, m) 1.26 (1H, m)	21.3	1.31 (1H, m) 1.22 (1H, m)	20.5
12′	1.96 (1H, m) 1.18 (1H, m)	39.7	2.00 (1H, m) 1.16 (1H, m)	40.2	1.92 (1H, m) 1.12 (1H, m)	39.5
13′		42.9		43.9		43.0
14′	1.38 (1H, m)	50.6	1.24 (1H, m)	55.9	1.17 (1H, m)	55.2
15′	1.62 (1H, m) 1.12 (1H, m)	23.8	1.82 (1H, m) 1.48 (1H, m)	27.0	1.90 (1H, m) 1.34 (1H, m)	26.9
16′	1.90 (1H, m) 1.32 (1H, m)	28.3	1.90 (1H, m) 1.48 (1H, m)	28.8	1.74 (1H, m) 1.21 (1H, m)	28.1
17′	1.14 (1H, m)	55.9	1.08 (1H, m)	55.0	1.01 (1H, m)	54.7
18′	0.66 (3H, s)	11.9	0.67 (3H, s)	12.3	0.61 (3H, s)	11.9

19′	0.90 (3H, s)	22.9	0.93 (3H, s)	23.5	1.01 (3H, s)	25.3
20′	1.45 (1H, m)	35.5	1.45 (1H, m)	35.3	1.34 (1H, m)	34.8
21′	0.94 (1H, d, 6.5)	18.4	0.94 (1H, d, 6.5)	18.5	0.88 (1H, d, 6.5)	18.4
22′	1.80 (1H, m) 1.35 (1H, m)	30.9	1.81 (1H, m) 1.37 (1H, m)	31.0	1.67 (1H, m) 1.19 (1H, m)	31.1
23′	2.39 (1H, m) 2.25 (1H, m)	30.9	2.39 (1H, m) 2.25 (1H, m)	30.8	2.20 (1H, m) 2.08 (1H, m)	30.9
24′		179.0		178.2		175.2

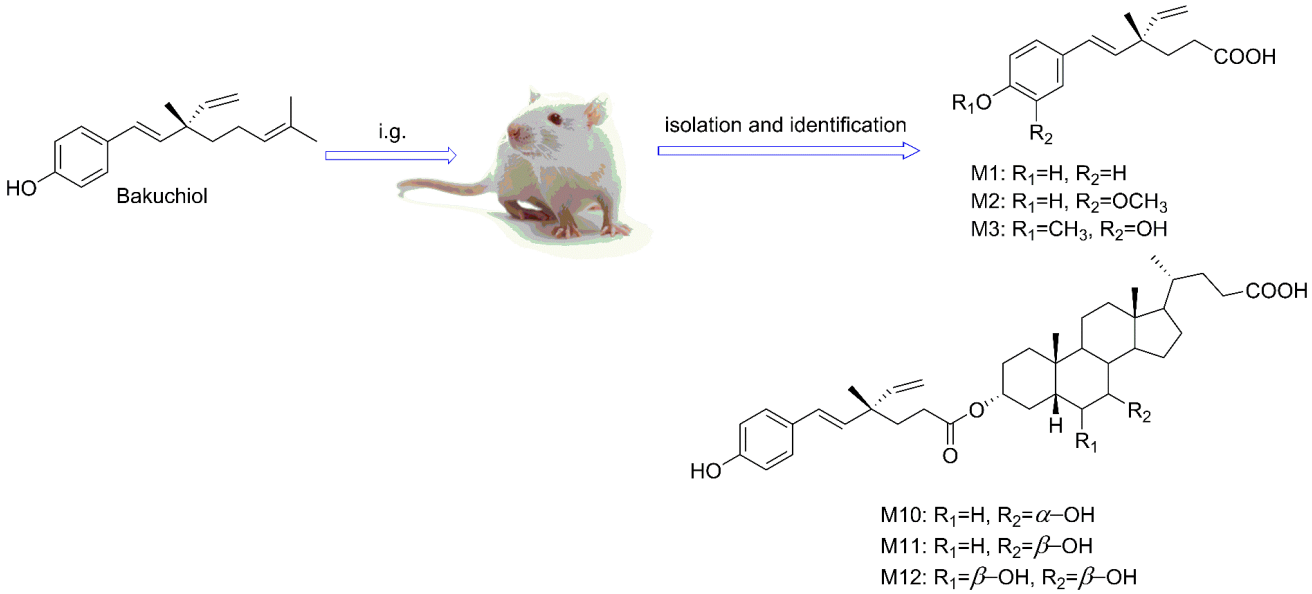

Graphical abstract